

See discussions, stats, and author profiles for this publication at: <https://www.researchgate.net/publication/228343598>

Value of information and experimentation in milling profit optimisation

Article in *International Journal of Mechatronics and Manufacturing Systems* · September 2009

DOI: 10.1504/IJMMS.2009.028082

CITATIONS

5

READS

62

4 authors, including:



[Raul Zapata](#)

United States Navy

20 PUBLICATIONS 81 CITATIONS

[SEE PROFILE](#)



[Tony L. Schmitz](#)

University of North Carolina at Charlotte

254 PUBLICATIONS 2,714 CITATIONS

[SEE PROFILE](#)

Value of information and experimentation in milling profit optimisation

R.E. Zapata-Ramos* and T.L. Schmitz

Machine Tool Research Center,
Department of Mechanical and Aerospace Engineering,
University of Florida,
237 MAE-B, Gainesville, FL 32611, USA
Fax: (352) 392-1071
E-mail: quique@ufl.edu
E-mail: tschmitz@ufl.edu
*Corresponding author

M. Traverso

Department of Industrial and Enterprise Systems Engineering,
University of Illinois at Urbana-Champaign,
8 Florida Drive, Urbana, IL 61801, USA
E-mail: mtraver2@uiuc.edu

A. Abbas

Information Systems and Decision Analysis Lab (ISDAL),
Department of Industrial and Enterprise Systems Engineering,
University of Illinois at Urbana-Champaign,
117 Transportation Building,
MC-238, Urbana, IL 61801, USA
Fax: (217) 244-5705
E-mail: aliabbas@uiuc.edu

Abstract: This paper presents a decision-analytic approach to milling optimisation in the presence of uncertainty. The decisions include the milling parameter settings and the uncertainties include the probability of stability and tool life. We quantify the stability uncertainty by Monte Carlo simulation, where the force model coefficients and frequency response function uncertainties are propagated through the stability model. We treat tool life uncertainty using encoding. We then apply a single attribute objective function, expected profit, to determine optimal settings. Using this formulation, we determine the value of an experiment, the optimal experiment settings, and the value of perfect information.

Keywords: milling; optimisation; decision analysis; stability lobe diagram; uncertainty; value of perfect information; value of experiment.

Reference to this paper should be made as follows: Zapata-Ramos, R.E., Schmitz, T.L., Traverso, M. and Abbas, A. (2009) 'Value of information and experimentation in milling profit optimisation', *Int. J. Mechatronics and Manufacturing Systems*, Vol. 2, Nos. 5/6, pp.580–599.

Biographical notes: Raúl Zapata-Ramos is pursuing his PhD student at the Machine Tool Research Center within the University of Florida's Department of Mechanical and Aerospace engineering. He received his BS Degree from the University of Puerto Rico, Mayaguez Campus, and his MS Degree from the University of Florida. His primary research interests are machine tool accuracy and the optimisation of machining process parameter selection.

Tony L. Schmitz is an Associate Professor in the Department of Mechanical and Aerospace Engineering at the University of Florida, where he is director of the Machine Tool Research Center. His primary research interest is precision manufacturing. Prior appointments include a post-doctoral fellowship at the National Institute of Standards and Technology, Gaithersburg, MD and Lecturer at Johns Hopkins University, Baltimore, MD. Recent recognitions include the National Science Foundation CAREER award, Office of Naval Research Young Investigator award, and the Society of Manufacturing Engineers Outstanding Young Manufacturing Engineer award. He received his PhD from the University of Florida in 1999.

Michael Traverso is an undergraduate student in Industrial Engineering in the Department of Industrial and Enterprise Systems Engineering at the University of Illinois at Urbana-Champaign. His primary research interests include optimisation under uncertainty and the organisation and design of complex systems.

Ali E. Abbas is an Assistant Professor in the Department of Industrial and Enterprise Systems Engineering at the University of Illinois at Urbana-Champaign (UIUC). His research interests include decision-making under uncertainty and information theory. He received his PhD in Management Science and Engineering in 2003 (PhD minor in Electrical Engineering) from Stanford University. He joined UIUC in 2004 and previously worked in Schlumberger Oilfield Services, where he held positions in wireline logging, operations management, and international training. He is a senior member of IEEE and a member of the Decision Analysis Council at INFORMS.

1 Introduction

1.1 *Smart machining*

Smart machine tools is an emerging research field that has been identified as a key technology for enabling first part correct machining in an environment of high accuracy requirements, shortened time to market, and greater product variability, as defined in Corbett (1998). John Kohls, affiliated with the Smart Machine Platform Initiative (a partnership between numerous manufacturers, TechSolve, and Benét Laboratories as described on the SMPI website), provides a definition of smart machines in Teresko (2007).

“A smart machine is one that can *make decisions* about the manufacturing process in real time. A smart machine knows itself. It is one that understands how to make a part. It can monitor, diagnose and correct when deviations occur. And it can learn for *optimizing* in the future.” [Emphasis added by the authors]

A similar description is proposed by the Smart Machining Systems programme at the National Institute of Standards and Technology, Gaithersburg, MD. In this programme, the role of smart machines, as defined on the NIST Manufacturing Engineering Laboratory website, is to “enable cost effective manufacture of first and every part to specification and on schedule”. The following is also stated on the programme’s website.

“Such systems will complement and enhance the skills of machine operators, process planners and design engineers in the manufacturing enterprise by sharing the knowledge and information among these functions to *optimize* the design and manufacturing processes to their fullest.” [Emphasis added by the authors]

Given these objectives, it is clear that the important features of a smart machine include:

- collection of relevant process and machine information in a concise format
- a framework for rational decision making based on the available data, appropriate models and the user’s preferences
- incorporation of uncertainty into the decision-making process.

Naturally, profit maximisation, is a primary consideration as well.

Because decision-making, as highlighted by Kohls in Teresko (2007), is a key aspect of smart machining systems, the concepts of decision theory are integral to the successful development of this technology. Decision theory applies discrete (and continuous) mathematics to model decision making in all activities, including science and engineering. In the normative or prescriptive approach, it defines how ideal decision-makers should make decisions and how optimal decisions can be reached, even in the presence of uncertainty. Decision analysis is the practical application of normative decision making to actual situations.

1.2 Application of decision analysis

In this paper, we apply decision analysis fundamentals to milling profit optimisation. This builds on our recent efforts detailed in Abbas et al. (2007), which provided us with a basis for including uncertainties in the milling process. By optimising profit and including the influence of the process dynamics (on, e.g., stability, surface location error, and surface roughness) as constraints rather than as objectives, we implemented a comprehensive approach to milling optimisation. We concentrated on observing the encoded uncertainties in FMCs and tool life in profit calculation.

Other studies in milling optimisation have explored the use of multiple objectives and various optimisation methods. Early efforts in this field include Boothroyd and Rusek (1976), Gilbert (1950), Okushima and Hitomi (1964), Tee et al. (1969) and Wu and Ermer (1966). Much of the prior work such as Beightler and Philips (1970), Walvekar and Lambert (1970), Ermer (1971), Hati and Rao (1976), Giardini et al. (1988), Sheikh et al. (1980), Petropoulos (1975), Eskicioglu et al. (1985), Lambert and Walvekar (1978), Jha (1990), Gopalakrishnak and Al-Khayyal (1991), Armarego et al. (1993, 1994),

Sonmez et al. (1999), Wang and Armarego (2001), Lin (2002), Kim et al. (2002), Juan et al. (2003) and Lu et al. (2003), has focused on a single aspect of milling productivity, such as tool wear or material removal rate, while the influence of the process dynamics has not typically been considered. However, the approach used in Abbas et al. (2007) adopts a more holistic view that can consider multiple constraints, including stability, surface location error, surface roughness, which depend on the process dynamics, and tool life, while maximising what we believe to be the most appropriate single objective function, profit.

Current research involves improving our knowledge of the uncertain system through experimentation. This requires us to first express our uncertainty about the stability of the system under given parameter settings. Traditionally, the stability boundary is considered to be a 'step function' that is stable below and unstable above. However, by incorporating uncertainties in the FMCs and the tool-holder-spindle-machine FRF, we can now provide an infinite set of stability boundaries, each with a certain probability. We present simulation results here to determine the cumulative probability of stability vs. axial depth of cut at any given spindle speed setting.

We frame milling optimisation as a decision problem with uncertainty in the stability limit and tool life. We calculate the optimal milling setting given these uncertainties and also determine the value of perfect information on the location of the stability boundary. This value of perfect information provides an upper limit to the value of any information gathering activity, about the boundary in this case. We then calculate the value of an experiment that determines whether the boundary is above or below a given axial depth. Naturally, the value of this experiment will be less than the value of perfect information since it does not locate the actual position of the boundary, but only provides refinement about its position. Finally, we compare the value of this experiment to the value of perfect information.

The paper is structured as follows. Section 2 outlines a method to quantify the stability uncertainty. Section 3 describes the profit calculation at a given setting. Section 4 presents a decision-analytic model for optimising profit, taking into account the uncertainty about stability and provides a theoretical analysis of the value of experiment using Bayesian updating. A numerical example is presented in Section 5. In Section 6, we present conclusions and future work.

2 Quantifying the stability uncertainty

Determining the milling stability uncertainty is notably different from obtaining the distributions of the uncertainties for the analysis inputs, such as the distribution of FMCs and Frequency Response Function (FRF) of the tool-holder-spindle-machine assembly, as reflected at the tool point. For our purposes, we assume that estimates of the FMCs are based on experience or tabulated values, while the FRF is measured.¹ The stability limit, on the other hand, is obtained from calculations based on the inputs (and the milling model). The stability uncertainty therefore depends on the input values (FMCs and FRF), their propagation through the stability model and the selected operating point. Note that uncertainty in the milling model itself was not considered at this stage.

In this research, we apply the frequency domain, analytical stability analysis described in Altintas (2000) and Altintas and Budak (1995) to determine the stability limit. Inputs to this algorithm include the radial depth of cut and number of cutter teeth (deterministic decisions), the FRF (uncertain) and the FMCs (uncertain). The output is the well-known stability lobe diagram, which identifies the stability boundary (i.e., the allowable axial depth of cut without chatter) as a function of spindle speed. The traditional first order Taylor series expansion method for evaluating measurement uncertainty, as described in ISO (1993) and Taylor and Kuyatt (1994), is not conveniently applied in this instance. Therefore, a Monte Carlo approach was used Duncan et al. (2006).

In the Monte Carlo simulation, the FMCs and FRF uncertainties are quantified using appropriate mean and standard deviation values for the selected distributions (Table 1). The FMCs are scalar values and the uncertainty could be evaluated by a number of methods. In this case, the FMCs uncertainty is determined through encoding, a decision analysis approach based on the user's experience and beliefs. The frequency dependent, complex valued FRF is determined by measurement. Due to its bivariate (complex valued) nature, its uncertainty evaluation is complicated. A separate study Kim and Schmitz (2007) determined that the primary uncertainty contributors for impact testing, which are commonly applied to measure the tool point FRF, are the calibration coefficients of the measurement transducers, typically an impact hammer and accelerometer. To include the calibration coefficients uncertainties, they were first extracted from the scaled FRF prior to using the FRF in the Monte Carlo simulation. The uncertainty in the hammer and accelerometer calibration coefficients was then introduced by multiplying randomly sampled values of the coefficients by the unscaled FRF. The uncertainty due to measurement repeatability was also considered. The repeatability was introduced through a frequency dependent scaling of the FRF. The scaling factors were random samples of a Gaussian distribution with a mean of zero and a standard deviation of 0.35% multiplied by the value of the FRF at each frequency value.

The relative influence of the FMCs and FRF uncertainties were compared using the Monte Carlo simulation. The Gaussian distributions and the mean/standard deviation values provided in Table 1 were applied. Figure 1 shows the two standard deviation intervals obtained from the Monte Carlo simulation for the cases of:

- FRF uncertainty only
- FMCs uncertainty only.

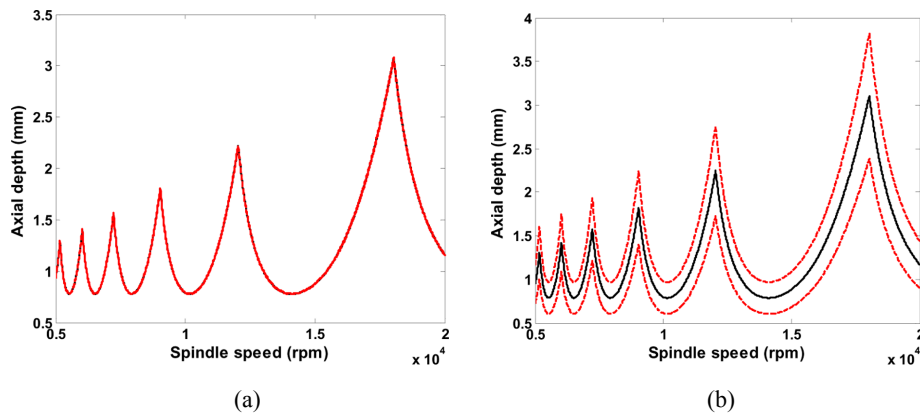
Because the FMCs uncertainty dominates for the selected values, the FRF uncertainty is not considered in the remainder of this study. The simulation used a 50% radial immersion (radial depth equal to the cutter radius), two cutting teeth and the FRF was constructed using a single degree of freedom model with a stiffness of $k = 1.6 \times 10^{-7}$ N/m, a damping ratio of $\zeta = 0.05$ and a natural frequency of $\omega_n = 2400 \cdot 2\pi$ rad/s (or 2400 Hz). The FRF was described using equation (1), where ω is the excitation frequency (rad/s).

$$FRF = \frac{1}{k} \left(\frac{\omega_n^2}{\omega_n^2 - \omega^2 + i2\zeta\omega_n\omega} \right) \tag{1}$$

Table 1 FMCs and FRF uncertainties

Quantity	Mean	Standard deviation	Units
Force model coefficient (radial)	900	100	N/mm ²
Force model coefficient (tangential)	3000	333.3	N/mm ²
Hammer coefficient	926	0.009	N/V
Accelerometer coefficient	1027	0.0033	m/s ² /V

Figure 1 Two standard deviation intervals for: (a) FRF uncertainty only; and (b) Force Model Coefficient (FMC) uncertainty only. Gaussian distributions were assumed for all inputs (see online version for colours)



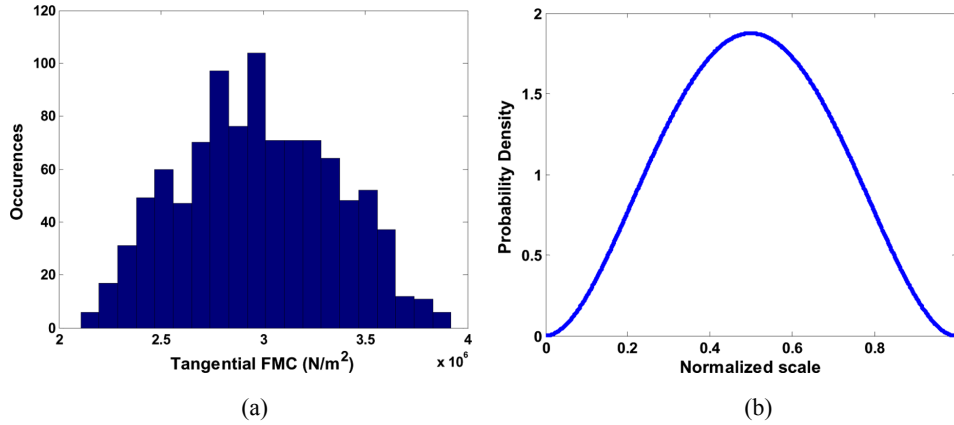
In most cases, assuming Gaussian, or normal, distributions for the uncertainties is reasonable unless other information is available. In decision analysis, however, the uncertainty distributions must accurately reflect the users’ beliefs, which may tend away from Gaussian. In this regard, beta distributions provide significant flexibility in shape and location. Similarly, due to the nature of the stability analysis in Altintas (2000) and Altintas and Budak (1995), there is no guarantee that the output will be Gaussian, so a beta distribution was selected to describe the output as well. Beta distributions are defined on a domain of x_{\min} to x_{\max} using two parameters r and k , as shown in the probability density function provided in equation (2):

$$f(x | x_{\min}, x_{\max}, r, k) = B(x - x_{\min})^{r-1} (x_{\max} - x)^{k-1}, x_{\min} < x < x_{\max} \tag{2}$$

where B is a scaled Beta function with parameters x_{\min} , x_{\max} , r , and k .

Using beta distribution, it is possible to quantify the stability behaviour, given uncertain inputs. For example, using an appropriately scaled beta distribution with beta function parameters, (r, k) , of $(3, 3)$ for the FMCs, we randomly sampled 1000 values to obtain the histogram shown in Figure 2.

Figure 2 Histogram of the selected values of the tangential Force Model Coefficient (FMC) from a scaled (3, 3): (a) beta distribution and (b) beta distribution with parameters (3, 3) (see online version for colours)



In this study, we assumed perfect correlation between the tangential and radial FMCs. Therefore, only the tangential value was sampled in the Monte Carlo simulation and the radial value was taken to be proportional (equal to 0.3 times the tangential coefficient). Table 2 shows the additional simulation input data. The 1000 paired values of the FMCs were propagated through the stability model to obtain 1000 stability boundaries (Figure 3). The Monte Carlo output provided a distribution of stability boundaries at every spindle speed. For example, a histogram of the distribution at 18,000 rpm is provided in Figure 4. In this study, the distributions were the same at each spindle speed, but this is not necessarily the case if FRF uncertainty is included. Fitting the Figure 4 histogram (once normalised) to a beta distribution using maximum likelihood estimates of the parameters yielded a beta distribution with parameters ($x_{\min} = 2$ mm, $x_{\max} = 3.8$ mm, $r = 1.76$, and $k = 2.56$). See Figure 5 for a normalised version of a beta distribution with these parameters.

Table 2 Inputs to the Monte Carlo stability simulation

<i>Parameter</i>	<i>Value</i>	<i>Units</i>
Stiffness	1.6×10^7	N/m
Damping ratio	0.05	–
Natural frequency	2400	Hz
Number of teeth	4	–
Radial immersion	50%	–
Tangential force model coefficient	3000 ± 1000	N/mm ²
Radial force model coefficient	900 ± 300	N/mm ²

In order to normalise the ranges for the FMCs so that they relate to the beta distribution (since beta distributions are defined only from 0 to 1), the lowest value in the FMC range is normalised to a positive value very close to 0. On the other hand, the upper bound of the range is normalised to a value just less than 1.

Figure 3 Result of the Monte Carlo stability simulation. The band is composed of 1000 different stability boundaries that each depends on the random selection of force model coefficients (see online version for colours)

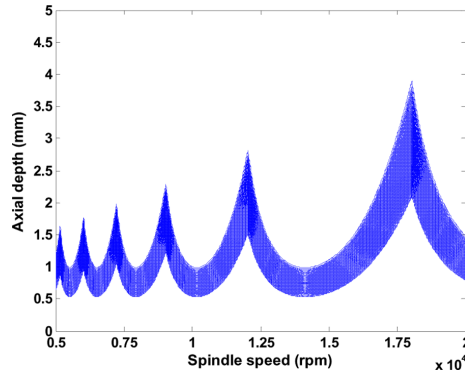


Figure 4 Histogram of the stability limits at 18,000 rpm from Monte Carlo simulation. Calculations show that this histogram (once normalised) is best fit by a beta distribution with parameters (1.76, 2.65) (see online version for colours)

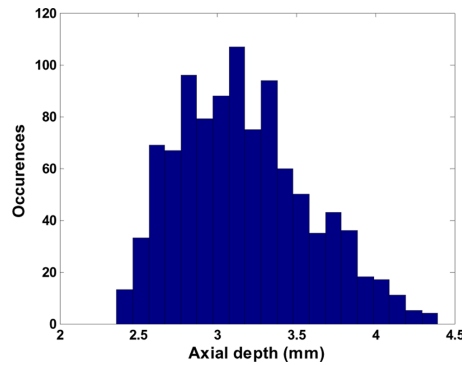
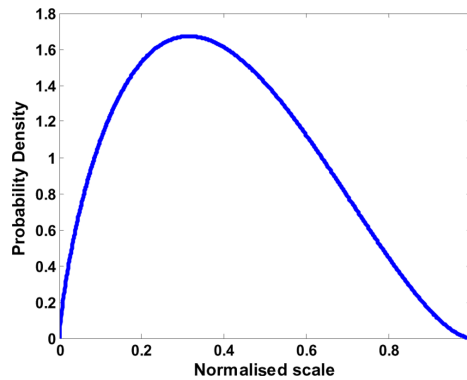


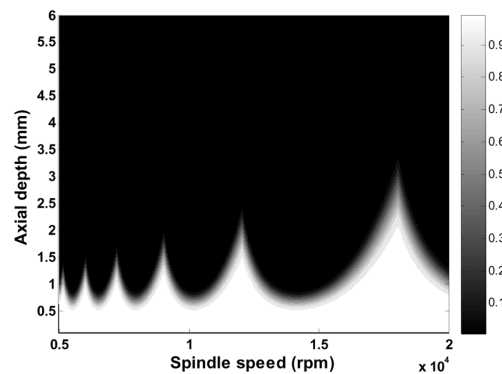
Figure 5 Example beta distribution with parameters (1.76, 2.56) that was fit to the Figure 4 histogram using a maximum likelihood method from Bernardo and Smith (2000) (see online version for colours)



The value of the cumulative distribution at any combination of axial depth and spindle speed within the axial depth range of the 1000 stability boundaries obtained from

simulation provides the probability that the ‘true’ stability boundary is at a lower axial depth (i.e., the likelihood that the selected parameter combination is unstable). The likelihood that the parameter set s is stable, or the probability of stability, $p(\text{stab} | s)$, is determined by subtracting the probability of instability from one. Given that the beta distribution is a bounded distribution the remainder of the parameter space must be composed of valid probability values. Therefore, everything below the minimum of the beta distribution fit to the stability boundaries at each spindle speed is designated stable with $p(\text{stab} | s) = 1$ and everything above the maximum is unstable with $p(\text{stab} | s) = 0$. The results of the probability of stability calculations are provided in Figure 6. The probability of stability is finally used to calculate profit by multiplying the probability by the unconstrained value of profit at each parameters set.

Figure 6 Contour plot of the probability of stability calculated using the cumulative distribution function for each spindle speed value



3 Calculating profit at a given setting

In this section, we illustrate how to determine the profit at any given parameter setting (spindle speed and axial depth) if the process is stable. If the process is unstable at a given setting, we assume that the profit is zero (i.e., we ignore the possibility of reworking a part). We incorporate two uncertainties, process stability and tool life uncertainty. For any given tool setting we, therefore, first calculate the profit at that selected setting with a given value of tool life, $P(T, s)$. We then calculate the expected profit (expectation taken with respect to tool life) at the selected setting assuming the process is stable, which we denote as $P(s)$. We then calculate the expected profit at a given setting by multiplying the profit, $P(s)$, by the probability of stability at this setting.

To characterise the uncertainty in tool life, we use the same discretisation method applied in Abbas et al. (2007) and McNamee and Celona (2001), which preserves the first moment of the continuous distribution. This approach requires the user to perform a probability encoding exercise on the tool life. The user provides three values for this uncertainty, corresponding to the points of the variable of interest that have cumulative probabilities of 0.1, 0.5, and 0.9. We refer to these points as the Low, Base, and High points, respectively. For example, we denote the Low, Base, and High values for tool life as T_{Low} , T_{Base} and T_{High} , respectively, and observe that they have cumulative probabilities 0.1, 0.5 and 0.9. Once the Low, Base, and High values are determined,

we assign them discrete probabilities of occurrence equal to 0.25, 0.5 and 0.25, respectively (see McNamee and Celona (2001) for more details about this approach).

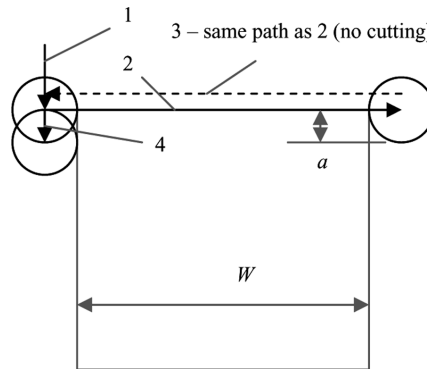
The profit at a given setting, $P(T, s)$ is the difference between revenue R and the cost of machining at that setting, $c_m(T, s)$. (See equation (3)).

$$P(T, s) = R - c_m(T, s). \tag{3}$$

Note that revenue is not a function of T or s and it is user defined. In this case, revenue was obtained using the cutting tool manufacturer’s suggested operating speed at the maximum allowable axial depth given the mean values of the FMCs and FRF in Table 2. We applied the tool life model described in Tsai et al. (2005) for this study. However, no suggested operating parameters were available, so a tool was selected from with geometry and composition that most closely resembled the tool used in Tsai et al. (2005) (R216.34-10045-AC22N tool, p.A148, of the Sandvik Coromant Rotating Tools and Inserts Handbook, 2006). This enabled us to use the suggested operating conditions from the manufacturer. The maximum allowable axial depth, obtained by applying the mean values of the FMCs to determine the stability boundary from simulation, and other cutting parameters were then used in simulation at a variety of feed per tooth values to determine the lowest test part cost. Although the mean values of the FMCs were not the same as those provided in Table 1, they (2395 N/mm² in the tangential direction, Rotating Tools and Inserts Handbook, 2006) were within two standard deviations of the Table 1 listings.

The test part consisted of machining away a 500 mm cube of material. The procedure for machining the part is as shown in Figure 7, where $W = 500$ mm. The tool moves into position adjacent to the part (1), translates relative to the part at the required radial depth, a , and axial depth to remove material (2), returns to its position (no cutting on the return path) (3) and, finally, moves on to the next radial depth location. This procedure is repeated until the entire layer is removed and starts over at the next layer until the entire block is machined away.

Figure 7 Diagram of the machining strategy for a single layer of the cube



The cost of machining $C_m(T, s)$ is obtained using equation (4), where t_m is the machining time, t_c is the cutting time, r_m is the cost of machining per unit time (\$1 per minute), t_{ch} is the time it takes for a tool change (4 s), C_t is the cost of a tool (\$114) and T is the tool life as determined from the Taylor-type tool life model described by equation (9) (obtained using the data provided in Tsai et al. (2005)).

$$C_m(T, s) = t_m r_m + (t_{ch} r_m + C_t) \frac{t_c}{T} \quad (4)$$

The values used to calculate t_m and t_c are shown in equations (5)–(8). In these equations, L is the total length of the tool path, L_c is the cutting portion of the tool path, and f is the feed rate in mm/min. The axial depth of cut is b and d is the diameter of the tool. In equation (9), v is the cutting speed (m/min) and f_t is the feed per tooth (mm/tooth).

$$t_m = \frac{L}{F} \quad (5)$$

$$t_c = \frac{L_c}{f} = \frac{L_c}{L} t_m \quad (6)$$

$$L = \frac{W}{b} \left(\frac{2W}{a} (W + d) + W \right) \quad (7)$$

$$L_c = \frac{W}{b} \left(\frac{W}{a} (W + d) \right) \quad (8)$$

$$T = 19.9549 \times 10^6 v^{-1.6265} f_t^{-0.1024} b^{-0.2837} \quad (9)$$

The values for tool life from equation (9) are used as the base value of tool life. At each operating point, the previously encoded values of tool life are used to scale the calculated tool life and obtain the low and high values for the cost calculation. These are then incorporated into the profit calculation in equation (3). Finally, we obtain the ideal profit of milling with setting s using equation (10).

$$P(s) = 25\% \times P(T_{\text{Low}}, s) + 50\% \times P(T_{\text{Base}}, s) + 25\% \times P(T_{\text{High}}, s). \quad (10)$$

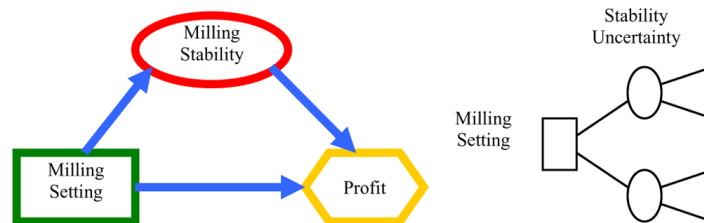
4 Milling optimisation and experimentation with uncertainty about stability

4.1 Value with no experimentation

Having characterised the stability and tool life uncertainties, as well as the profit, at a given setting, we now present a decision analytic model for milling optimisation. Figure 8 shows the basic decision diagram, as described in Howard and Matheson (1984, 2004) and a generic decision tree for this model. The diagram has three nodes. The decision node, ‘Milling Setting’ characterises the two decisions: spindle speed and axial depth of cut. The oval, ‘Milling Stability’, represents our uncertainty about stability at a given setting. The hexagon is the objective function, ‘Profit’. The user needs to make the optimal milling setting decision that maximises the expected value of profit, given the uncertainty about stability. The arrow in the diagram from Milling Setting to Milling Stability implies the probability of stability is influenced by the choice of the spindle speed and axial depth of cut. The arrows from Milling Setting and Milling Stability

into profit imply that both these factors influence the expected profit. A generic decision tree is shown to the right of the figure, where Milling Setting decisions are represented by a square, and uncertainty of stability is represented by circles.

Figure 8 Decision diagram and generic decision tree for milling (see online version for colours)



In the remaining sections of the paper, we denote spindle speed as ss and axial depth of cut as b . Assuming that the profit is zero when the milling conditions are unstable, we can calculate the optimal profit P^* using the following formula:

$$P^* = \max \{P(s)p(\text{stab} | s)\} \tag{11}$$

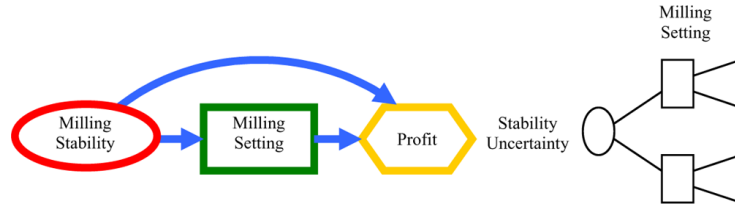
where P^* represents the maximum expected value of profit that can be obtained given the current state of information about the true stability boundary while considering the uncertainty in tool life and its effect on profit. At any given setting, the milling operation could be stable or unstable due to the uncertainty about the stability boundary. If the user knew the boundary was higher, he or she would choose a different setting than this setting. Therefore, since this information can be refined by experimentation or information gathering, we call this profit value, P^* , the value with no further information.

4.2 Value with perfect information

The value of perfect information is the maximum amount the user would be willing to pay to get information about the true location of the stability boundary. For a risk-neutral decision-maker (one who values uncertain deals at their expected value), the value of perfect information is equal to the difference between the value of the deal with perfect information and the value of the deal with no information. The value of perfect information about the location of the contour is also the upper bound on any information gathering activity about the location of the contour. For example, we will show how an experiment determines an interval for the location of the stability boundary, because of which the value of the experiment must be less than the value of perfect information.

In milling, if we knew exactly where the stability boundary is, we could tell immediately what the profit would be at a given setting (either zero or $P(s)$). In effect, this means we are optimising with perfect information about the location of the stability boundaries. Figure 9 shows the decision diagram and generic decision tree for this situation. Note that there is an arrow from Milling Stability uncertainty into Milling Setting decision, implying that we have perfect knowledge of whether or not we will have stability at a given milling setting.

Figure 9 Decision diagram and generic decision tree for optimisation with perfect information about the stability boundary (see online version for colours)



To calculate the value of the deal with perfect information about the stability boundary, we determine the optimal profit that can be obtained for each location of the stability boundary and multiply it by the probability that the boundary is actually at the location.

We calculate the optimal profit with perfect information P^I using equation (12).

$$P^I = E[\max P(s) | \text{PerfectInformation}]. \tag{12}$$

Here, E is the expectation with respect to the location of the stability limit. The difference $P^I - P^*$ is the value of perfect information if a decision maker is risk-neutral. While it might not always be feasible to obtain perfect information, its value has an important significance as the upper bound on any information gathering activity about the uncertainty of interest.

4.3 Value of experimentation

Experiments are generally conducted to obtain partial information about the system in question when perfect information is either difficult (sometimes impossible) to obtain or is too costly. As we mentioned, the value of this partial information is never as high as the value of perfect information, but may be significant nonetheless. In effect, the value of experimentation can even provide us with insights as to whether or not proceeding with experimentation is feasible. For example, if the value of the experiment is less than the cost of the experiment the user may wish to proceed with his current state of information rather than waste time and money performing the experiment.

Suppose we can conduct an experiment (such as a cutting test or a series of cutting tests) that would tell us whether or not the system is stable at a given spindle speed, ss_0 , and axial depth, b_0 . In addition, assume that the cumulative probability of stability is at this setting is p_0 . i.e., $p(ss_0, b_0) = p_0$. If the experiment at (ss_0, b_0) turns out to be stable, then the stability limit must be located at an axial depth higher than b_0 at the spindle speed ss_0 . i.e., the milling at (ss_0, b_1) , with $b_1 \leq b_0$ must also be table. In effect this observation enables us to update our probability of stability to be equal to one at any point (ss_0, b_1) , with $b_1 \leq b_0$. However, we still do not know the stability limit at the spindle speed ss_0 . In effect, the posterior distribution for probability of stability becomes

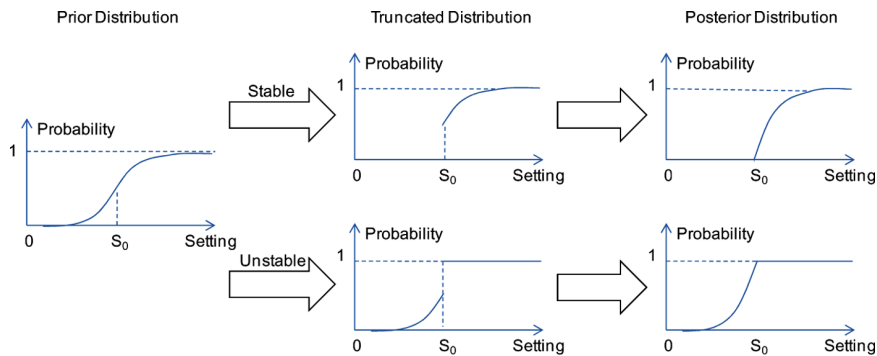
$$p_1(\text{stab} | ss_0, b_1) = \begin{cases} 1 & \text{for } b_1 \leq b_0 \\ \frac{p(\text{stab} | ss_0, b_1)}{p(\text{stab} | ss_0, b_0)} & \text{for } b_1 > b_0 \end{cases} \tag{13}$$

On the other hand, if the experiment at (ss_0, b_0) us unstable, then the stability limit must be lower than this point. Then the posterior probability is

$$p_1(\text{stab} | ss_0, b_1) = \begin{cases} 0 & b_1 \geq b_0 \\ \frac{p(\text{stab} | ss_0, b_1) - p(\text{stab} | ss_0, b_0)}{1 - p(\text{stab} | ss_0, b_0)} & b_1 < b_0 \end{cases} \quad (14)$$

Figure 10 shows this updating graphically.

Figure 10 Bayesian updating of probability of stability. The curves indicate the cumulative probability of stability vs. axial depth. Here, S_0 is the setting of the experiment (see online version for colours)



We are still uncertain about the location of the stability limit even after observing the results of the experiment. However, we have now narrowed the distribution of the uncertainty. Each stability boundary would be associated with a unique set of inputs (FMCs and tool point FRF) allowing the user to truncate the stability boundaries above or below the experimental parameter set depending on the results of the cutting test(s).

Based on these results, we have two decisions to make in this setting: the first is the optimal experimental setting and the second is the optimal milling setting, given the results of the experiment.

5 Numerical example for optimum experimentation

In this section, we calculate the expected profit at a given milling setting taking into account the stability uncertainty. We then calculate the value of perfect information and experimentation.

To calculate the value of perfect information, we selected 15 spindle speeds around the spindle speed of 18,033 rpm. We discretised the stability distribution at each spindle speed into 1000 equally probable points; this creates a set of 1000 stability limit contours. For each contour, we calculated:

- the maximum profit that could be obtained if it were the stability contour
- the probability that it is the stability limit.

This probability of occurrence each contour is simply 0.1%. We then multiplied the maximum profit by this probability and summed over all possible stability contours. This gave us the maximum expected profit that could be obtained with perfect information about the location of the contour. This was equal to \$29,812. Thus, the value of perfect information is equal to $\$29,812 - \$29,148 = \$664$. This is the upper bound on any information gathering activity about the location of the stability limit.

Next, we calculated the value of an experiment that determines whether or not it is stable at a given setting. Two decisions are involved:

- determining the optimal setting for an experiment
- determining where to mill given the results of the experiment.

To calculate the value of the experiment, we selected a spindle speed of 18,033 rpm.

We then selected several axial depths. For each axial depth, we calculated

- the probability of stability at this spindle speed
- the updated (posterior) distribution if the experiment indicated stable
- the optimal milling parameters if the experiment indicated stable, obtained using the new (posterior) probability of stability
- the updated (posterior) distribution if the experiment indicated unstable
- the optimal milling setting if the experiment indicated unstable, obtained using the new (posterior) probability of stability
- the expected value of profit by experimenting at this point and then milling given the test indication.

See Tables 3–5. We then determined the experiment setting that maximises this expected profit.

Table 3 The probability of stability for a selection of Spindle Speed (ss) and Axial Depth of Cut (ADOC) combinations

<i>ADOC/ss</i>	<i>17958</i>	<i>17973</i>	<i>17988</i>	<i>18003</i>	<i>18018</i>	<i>18033</i>	<i>18048</i>	<i>18063</i>
2.067	0.995	0.998	1.000	1.000	1.000	1.000	1.000	0.998
2.073	0.994	0.997	0.999	1.000	1.000	1.000	1.000	0.997
2.079	0.992	0.996	0.998	1.000	1.000	1.000	0.999	0.996
2.085	0.991	0.994	0.997	0.999	1.000	1.000	0.999	0.994
2.091	0.989	0.993	0.996	0.998	1.000	1.000	0.998	0.993
2.097	0.987	0.991	0.995	0.997	0.999	1.000	0.997	0.991
2.103	0.985	0.989	0.993	0.996	0.999	0.999	0.995	0.989
2.109	0.983	0.987	0.992	0.995	0.998	0.998	0.994	0.987
2.115	0.980	0.985	0.990	0.994	0.997	0.998	0.992	0.985
2.121	0.978	0.983	0.988	0.992	0.995	0.996	0.991	0.983

Table 4 Profit calculation for the same selection of spindle speed and axial depth combinations as in Table 3

<i>ADOC/ss</i>	<i>17958</i>	<i>17973</i>	<i>17988</i>	<i>18003</i>	<i>18018</i>	<i>18033</i>	<i>18048</i>	<i>18063</i>
2.067	\$29,115	\$29,116	\$29,117	\$29,117	\$29,118	\$29,118	\$29,119	\$29,120
2.073	\$29,123	\$29,124	\$29,125	\$29,125	\$29,126	\$29,126	\$29,127	\$29,127
2.079	\$29,131	\$29,132	\$29,132	\$29,133	\$29,134	\$29,134	\$29,135	\$29,135
2.085	\$29,139	\$29,140	\$29,140	\$29,141	\$29,141	\$29,142	\$29,142	\$29,143
2.091	\$29,147	\$29,147	\$29,148	\$29,149	\$29,149	\$29,150	\$29,150	\$29,151
2.097	\$29,155	\$29,155	\$29,156	\$29,156	\$29,157	\$29,157	\$29,158	\$29,159
2.103	\$29,162	\$29,163	\$29,163	\$29,164	\$29,165	\$29,165	\$29,166	\$29,166
2.109	\$29,170	\$29,170	\$29,171	\$29,172	\$29,172	\$29,173	\$29,173	\$29,174
2.115	\$29,178	\$29,178	\$29,179	\$29,179	\$29,180	\$29,180	\$29,181	\$29,181
2.121	\$29,185	\$29,186	\$29,186	\$29,187	\$29,187	\$29,188	\$29,188	\$29,189

Table 5 Expected profit for a selection of a spindle speed and axial depth combinations; the values are obtained by multiplying the corresponding entries in Tables 3 and 4. The maximum expected profit is equal to \$29,148 and occurs at a spindle speed of 18,033 rpm and axial depth of 2.0907 mm

<i>ADOC/ss</i>	<i>17958</i>	<i>17973</i>	<i>17988</i>	<i>18003</i>	<i>18018</i>	<i>18033</i>	<i>18048</i>	<i>18063</i>
2.067	\$28,977	\$29,053	\$29,102	\$29,117	\$29,118	\$29,118	\$29,118	\$29,056
2.073	\$28,944	\$29,031	\$29,092	\$29,124	\$29,126	\$29,126	\$29,119	\$29,034
2.079	\$28,907	\$29,004	\$29,077	\$29,122	\$29,134	\$29,134	\$29,112	\$29,006
2.085	\$28,865	\$28,972	\$29,056	\$29,114	\$29,141	\$29,142	\$29,099	\$28,975
2.091	\$28,819	\$28,936	\$29,031	\$29,100	\$29,142	\$29,148	\$29,081	\$28,939
2.097	\$28,770	\$28,896	\$29,000	\$29,081	\$29,135	\$29,147	\$29,058	\$28,898
2.103	\$28,717	\$28,852	\$28,966	\$29,057	\$29,123	\$29,140	\$29,030	\$28,854
2.109	\$28,660	\$28,804	\$28,927	\$29,028	\$29,106	\$29,126	\$28,998	\$28,806
2.115	\$28,600	\$28,752	\$28,885	\$28,995	\$29,083	\$29,107	\$28,961	\$28,754
2.121	\$28,536	\$28,697	\$28,838	\$28,958	\$29,056	\$29,084	\$28,921	\$28,699

The results indicate that we should experiment at a spindle speed of 18,033 rpm and axial depth of 2.64 mm. If the experiment indicates stability, use this point for the milling operation. If the experiment indicates instability, move to the operating point of spindle speed of 18,033 rpm and axial depth of 2.09 mm. By conducting an experiment first and then conducting the milling, we have an expected value of profit equal to \$29,505. The value of this experiment is, therefore, equal to $\$29,505 - \$29,148 = \$357$. Note that the value of this experiment is approximately half (53%) of the value of perfect information (or clairvoyance). See Figures 11 and 12.

Figure 11 Decision diagram and generic decision tree for experimentation (see online version for colours)

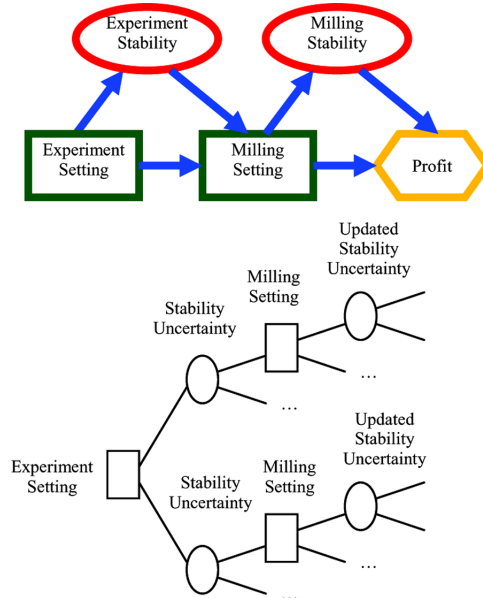
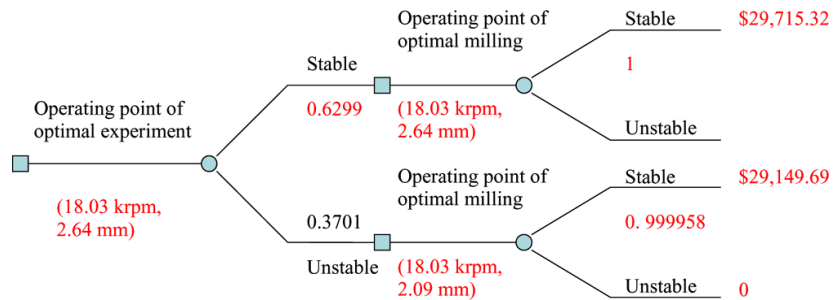


Figure 12 Optimal experiment and milling setting given the results of the experiment (see online version for colours)



6 Conclusions

We illustrated how to calculate the probability of stability in milling and then showed how decision-analysis could be used to calculate the optimal settings in the presence of uncertainty about the location of the stability limit. We also demonstrated how to calculate the value of perfect information and the value of an experiment. We illustrated how the value of perfect information provides an upper bound on the value of any information gathering activity about the stability of the milling. Based on a numerical example, we also illustrated how a simple binary experiment can provide approximately half the value of perfect information about the location of the contour. Furthermore, we illustrated how decision-analysis can be used to determine the optimal parameters of an experiment and how to determine the milling setting, given the results of the experiment. Future work can consider other types of experiments and the value they provide.

We believe that the techniques evaluated here will aid in the development of smart machines, which will require decision-making based on uncertain information gathered prior to or during the machining process. For example, we can incorporate the algorithms used in this paper to determine how to adjust the spindle speed or axial depth optimally if the milling is unstable. We can also calculate the value of a smart machining piece of equipment and price it according to its services with value-based pricing.

Acknowledgements

The authors gratefully acknowledge financial support for this work from the National Science Foundation (CMMI-0642569 and CMMI-0641827). They also wish to thank G. Hazelrigg for numerous helpful discussions and insights, M. Kurdi and R. Haftka for their contributions to the case study, and L. Yang for his time and contributions to the figures.

References

- Abbas, A., Yang, L., Zapata, R. and Schmitz, T. (2007) 'Application of decision analysis to milling profit maximization: an introduction', *Int. J. Materials and Product Technology*, Vol. 35, Nos. 1–2, pp.64–88.
- Altintas, Y. (2000) *Manufacturing Automation Metal Cutting Mechanics*, Machine Tool Vibrations, and CNC Design, Cambridge University Press, pp.45–46.
- Altintas, Y. and Budak, E. (1995) 'Analytical prediction of stability lobes in milling', *Annals of the CIRP*, Vol. 44, No. 1, pp.357–362.
- Armarego, E.J.A., Smith, A.J.R. and Wang, J. (1993) 'Constrained optimization strategies and CAM software for single-pass peripheral milling', *International Journal of Production Research*, Vol. 31, No. 9, pp.2139–2160.
- Armarego, E.J.A., Smith, A.J.R. and Wang, J. (1994) 'Computer-aided constrained optimization analyses and strategies for multi-pass helical tooth milling operations', *Annals of the CIRP*, Vol. 43, No. 1, p.437.
- Beightler, C.S. and Philips, D.T. (1970) 'Optimization in tool engineering using geometric programming', *AIE Transactions*, Vol. 2, pp.355–360.
- Bernardo, J.M. and Smith, A.F.M. (2000) *Bayesian Theory*, John Wiley & Sons, Ltd., Hoboken, NJ, pp.116, 460, 461.
- Boothroyd, G. and Rusek, P. (1976) 'Maximum rate of profit criteria in machining', *ASME Journal of Engineering for Industry*, Vol. 98, pp.217–220.
- Corbett, J. (1998) 'Smart machine tools', *Proceedings of the I MECH E Part I Journal of Systems and Control Engineering*, Vol. 212, No. 3, pp.203–213.
- Duncan, G.S., Tummond, M. and Schmitz, T. (2005) 'An investigation of the dynamic absorber effect in high-speed machining', *International Journal of Machine Tools and Manufacture*, Vol. 45, pp.497–507.
- Duncan, G.S., Kurdi, M., Schmitz, T. and Snyder, J. (2006) 'Uncertainty propagation for selected analytical milling stability limit analyses', *Transactions of NAMRI/SME*, Vol. 34, pp.17–24.
- Ermer, D. (1971) 'Optimization of the constrained machining economics problem by geometric programming', *ASME Journal of Engineering for Industry*, Vol. 93, pp.1067–1072.
- Eskicioglu, H., Nisli, M.S. and Kilic, S.E. (1985) 'An application of geometric programming to single-pass turning operations', *Proceedings of the International MTDR Conference*, Birmingham, pp.149–157.

- Giardini, C., Bugini, A. and Pagagnella, R. (1988) 'The optimal cutting conditions as a function of probability distribution function of tool life and experimental test numbers', *International Journal of Machine Tools and Manufacture*, Vol. 28, pp.453–459.
- Gilbert, W. (1950) 'Economics of machining', *Machining – Theory and Practice*, American Society for Metals, Metals Park, OH, pp.465–485.
- Gopalakrishnak, B. and Al-Khayyal, F. (1991) 'Machine parameter selection for turning with constraints: an analytical approach based on geometric programming', *International Journal of Production Research*, Vol. 29, pp.1897–1908.
- Hati, S.K. and Rao, S.S. (1976) 'Determination of optimum machining conditions – deterministic and probabilistic approaches', *ASME Journal of Engineering for Industry*, Vol. 98, pp.354–359.
- Howard, R.A. and Matheson, J.E. (Eds.) (1984) 'Influence diagrams', *The Principles and Applications of Decision Analysis, Strategic Decisions Group*, Menlo Park, CA, Vol. II, pp.721–762.
- Howard, R.A. and Matheson, J.E. (2005) 'Influence diagrams', *Decision Analysis*, Vol. 2, No. 3, pp.127–143.
- International Standards Organization (ISO) (1993) *Guide to the Expression of Uncertainty in Measurement* (Corrected and Reprinted 1995).
- Jha, N.K. (1990) 'A discrete database multiple objective optimization of milling operation through geometric programming', *Journal of Engineering for Industry*, Vol. 112, p.368.
- Juan, H., Yu, S.F. and Lee, B.Y. (2003) 'The optimal cutting-parameter selection of production cost in HSM for SKD61 tool steels', *International Journal of Machine Tools and Manufacture*, Vol. 43, pp.679–686.
- Kim, K-K., Kang, M-C., Kim, J-S., Jung, Y-H. and Kim, N-K. (2002) 'A study on the precision machinability of ball end milling by cutting speed optimization', *Journal of Materials Processing Technology*, Vols. 130–131, pp.357–362.
- Kim, H.S. and Schmitz, T. (2007) 'Bivariate uncertainty analysis for impact testing', *Measurement Science and Technology*, Vol. 18, pp.3565–3571.
- Lambert, B.K. and Walvekar, A.G. (1978) 'Optimization of multipass machining operations', *International Journal of Production Research*, Vol. 9, pp.247–259.
- Lin, T-R. (2002) 'Optimization technique for face milling stainless steel with multiple performance characteristics', *International Journal of Advanced Manufacturing Technology*, Vol. 19, pp.330–335.
- Lu, J., Ozdoganlar, O.B., Kapoor, S.G. and DeVor, R.E. (2003) 'A process-model based methodology for comprehensive process planning of contour turning operations', *Transactions of NAMRI/SME*, Vol. XXXI, pp.547–554.
- McNamee, P. and Celona, J. (2001) *Decision Analysis for the Professional*, 3rd ed., SmartOrg Inc., Menlo Park, CA.
- Okushima, K., and Hitomi, K. (1964) 'A study of economic machining: an analysis of the maximum-profit cutting speed', *International Journal of Production Research*, Vol. 3, No. 1, pp.73–78.
- Petropoulos, P.G. (1975) 'Optimal selection of machining rate variables by geometric programming', *International Journal of Production Research*, Vol. 13, pp.390–395.
- Rotating Tools and Inserts Handbook (2006) Sandvik Coromant, LIT-CAT 04-R, 08/04.
- Schmitz, T. (2000) 'Predicting high-speed machining dynamics by substructure analysis', *Annals of the CIRP*, Vol. 49, No. 1, pp.303–308.
- Schmitz, T., and Duncan, G.S. (2005) 'Three-component receptance coupling substructure analysis for tool point dynamics prediction', *Journal of Manufacturing Science and Engineering*, Vol. 127, No. 4, pp.781–790.

- Schmitz, T., Davies, M., and Kennedy, M. (2001a) 'Tool point frequency response prediction for high-speed machining by RCSA', *Journal of Manufacturing Science and Engineering*, Vol. 123, pp.700–707.
- Schmitz, T., Davies, M., Medicus, K., and Snyder, J. (2001b) 'Improving high-speed machining material removal rates by rapid dynamic analysis', *Annals of the CIRP*, Vol. 50, No. 1, pp. 263–268.
- Sheikh, A.K., Kendall, L.A. and Pandit, S.M. (1980) 'Probabilistic optimization of multitool machining operations', *ASME Journal of Engineering for Industry*, Vol. 102, pp.239–246.
- Sonmez, A.I., Baykasoglu, A., Turkay, D. and Filiz, I.H. (1999) 'Dynamic optimization of multi-pass milling operations via geometric programming', *International Journal of Machine Tools and Manufacture*, Vol. 39, No. 2, pp.297–320.
- Taylor, B.N. and Kuyatt, C.E. (1994) *Guidelines for Evaluating and Expressing the Uncertainty of NIST Measurement Results*, NIST Technical Note 1297 Edition.
- Tee, L., Ho, S. and DeVries, M. (1969) *Economic Machining Charts*, ASTM Paper No. MR 69-280.
- Teresko, J. (2007) 'Making machine tools smarter', *Industry Week*, 1 January, <http://www.industryweek.com/ReadArticle.aspx?ArticleID=13265>
- Tsai, M.K., Lee, B.Y. and Yu, S.F. (2005) 'A predicted modeling of tool life of high speed milling for SKD61 Tool Steel', *International Journal of Advanced Manufacturing Technology*, Vol. 26, p.711.
- Walvekar, A.G. and Lambert, B.K. (1970) 'An application of geometric programming to machining variable selection', *International Journal of Production Research*, Vol. 8, pp.241–245.
- Wang, J. and Armarego, E.J.A. (2001) 'Computer-aided optimization of multiple constraint single pass face milling operations', *Machining Science and Technology*, Vol. 5, No. 1, pp.77–99.
- Wu, S.M. and Ermer, D. (1966) 'Maximum profit as the criterion in the determination of the optimum cutting conditions', *ASME Journal of Engineering for Industry*, Vol. 88, pp.435–442.

Note

¹Alternately, the Force Model Coefficients could be determined from a separate set of measurements as shown by Altintas (2000) or the tool point FRF could be predicted as described in Schmitz and Duncan (2005), Duncan *et al.* (2005), Schmitz *et al.* (2001a, 2001b) and Schmitz (2000).

Websites

<http://www.mel.nist.gov/proj/sms.htm>

<http://www.techsolve.org/SMPI.php>